

MULTIMODAL IMAGING EVALUATION OF RABBIT MODELS

ASHLEY BROWN, VAN PHUC NGUYEN, IYABODE AJAYI, AND
YANNIS M. PAULUS

Currently available imaging modalities each have limitations in their scope, preventing a comprehensive view of the eye. A multimodal system can simultaneously use numerous modalities to increase the effectiveness of imaging to provide structural and functional information while decreasing the time and invasiveness of multiple procedures. In this study, optical coherence tomography (OCT), photoacoustic microscopy (PAM), fundus photography, fluorescein angiography (FA), and indocyanine green angiography (ICGA) were performed on a baseline rabbit model to verify the imaging system. Clear images distinguishing retinal vessels, choroidal vessels, and retinal layers were obtained, verifying the multimodal system's efficacy before imaging experimental models. Imaging macular degeneration and glaucoma animal models can advance understanding of novel treatments in ophthalmic research. Multimodal imaging also offers a promising new means for the early detection of retinal diseases in clinical settings.

Keywords

multimodal imaging, eye imaging, optical imaging, photoacoustic microscopy, optical coherence tomography, animal models

Introduction

Age-related macular degeneration (AMD) is the progressive aging of the macula, the part of the retina that allows you to see objects in your central vision. It is a leading cause of blindness and vision impairment in patients over 60 years old. As of 2019,

Contact: Ashley Brown <ashnb@umich.edu>
Van Phuc Nguyen
Iyabode Ajayi
Yannis M. Paulus

19.8 million people above the age of 50 in the United States have been diagnosed with AMD¹⁵. An additional study measured the direct cost of AMD diagnosis, treatment, and management in the United States at \$10 billion per year⁷. This cost does not include indirect medical expenses, such as home health care, nursing homes, additional vision aids, or productivity losses from being unable to work. Vision loss from AMD is currently irreversible, as retinal photoreceptors lack a regenerative capacity. However, regenerative cell therapies can offer a promising future treatment in restoring retinal function through transplanted stem cells¹.

Glaucoma is the second leading cause of blindness in the United States. As of 2020, an estimated 3 million Americans were living with glaucoma. Dangerously, around 50% of the 3 million people with this disease are undiagnosed due to little to no symptoms at the disease onset³. Symptoms of permanent vision loss tend to occur during late-stage disease progression once the patients have irreversible tunnel vision. In glaucoma, the aqueous humor, an optically clear fluid that nourishes and maintains the intraocular pressure (IOP) of the eye, begins to accumulate. This accumulation raises the IOP and irreversibly damages the optic nerve, causing progressive loss of peripheral to central vision. Current treatments involve topical eye drops or surgery to lower the IOP and prevent further vision loss. Unfortunately, these treatment options are not always financially accessible or fully effective. Topical medications can cost up to \$874 per year depending on the medication brand and prescribed regimen¹⁹, while surgery costs are dependent on an individual's insurance and come with increased risks of vision loss, bleeding, and infection⁵. Optical imaging could allow early disease detection and proactive treatment to slow or avoid vision loss completely.

Optical imaging is an important tool in clinical and research medical settings to diagnose patients and monitor treatment outcomes. Imaging can be used in the early-stage diagnosis and progressive monitoring of many eye diseases. In addition, longitudinal imaging can provide qualitative and quantitative insight on disease progression and evaluation of novel treatment techniques in developed animal models. There are currently a variety of available imaging systems; however, none can provide a high-resolution, three-dimensional image of the entire eye with a full anatomic and functional assessment. The most common techniques include fundus photography, fluorescein angiography (FA), indocyanine green angiography (ICGA), optical coherence tomography (OCT), and photoacoustic microscopy (PAM).

Fundus photography uses a low-power light microscope attached to a camera to provide a noninvasive, wide-field view of the interior surface of the eye¹³; however, it can be limited in image depth and cannot visualize the choroid. Fundus photography can be paired with FA to visualize the blood flow in the retina. This technique is commonly used to diagnose and monitor nonperfusion and

neovascularization¹². FA requires the intravenous injection of a fluorescent dye fluorescein sodium and thus is more invasive and holds risks of adverse side effects, including the risk of nausea, vomiting, anaphylaxis, and death.

ICGA allows visualization of the choroidal vessels using the exogenous contrast dye indocyanine green (ICG)¹¹. ICG is water-soluble and nontoxic. New blood vessels detected in the choroid could indicate macular degeneration or central serous chorioretinopathy¹³. Similar to FA, ICGA and ICG require the injection of an exogenous dye and only provide two-dimensional information.

OCT uses light waves to noninvasively produce a high-resolution, cross-sectional image of the retinal layers. This technique can be used to measure depth and evaluate changes in morphology to diagnose retinal diseases¹². OCT has limited ability to penetrate and evaluate deeper structures, such as the choroid, and cannot visualize leakage like FA and ICGA can. OCT angiography (OCTA) not only can visualize microvascular structures in the retina but also has limited ability to evaluate the choroidal vessels²⁴. Both OCT and OCTA currently have limited fields of view, although imaging technologies are expanding rapidly.

PAM is a nonionizing, noninvasive technique that utilizes a short-pulsed laser to produce light¹². The absorption of this light generates a sound that can be detected to create a high-resolution, high-depth image of deep biological tissues.

Each imaging technique has a variety of beneficial applications, but none can individually produce a high-resolution, three-dimensional image of the eye with a full anatomic and functional assessment. A multimodal imaging system could combine numerous imaging techniques, offsetting their individual limitations, to generate a comprehensive image of the eye. This would allow advanced early detection and progressive disease tracking in clinical and research settings.

Methods

To evaluate the rabbit model, this study used a multimodal imaging system consisting of OCT, PAM, fundus, FA, and ICGA. The use of a rabbit model was selected over the use of other rodent models as rabbits are phylogenetically closer to humans. Rabbit and human eyes share similarities in size, internal structures, choroidal blood supply, vitreous volume, and biochemical features. In addition, rabbit eyes have been previously studied to verify standardized values of fluid flow across the retina and retinal pigment epithelium (RPE). This paper focuses on imaging a baseline model, a group known to have no mutations or diseases, to obtain control data. The study was continued on both AMD and glaucoma experimental models following baseline system verification.

Animal Model

One New Zealand white rabbit (female, 9 months of age, weight 4 kg) was obtained for this study. All experiments were performed in compliance with the guidelines set by the Association for Research in Vision and Ophthalmology (ARVO) after the approval of protocol PRO00010288 from the University of Michigan's Institutional Animal Care and Use Committee (IACUC).

The rabbit was anesthetized 15 minutes prior to imaging with an intramuscular injection of ketamine (40 mg/kg) and xylazine (5 mg/kg). A local anesthetic of 0.5% topical proparacaine eye drops was also administered. Ten minutes prior to imaging, rabbit eyes were dilated with tropicamide 1% ophthalmic and phenylephrine hydrochloride 2.5% ophthalmic solution. The rabbit was kept on a water-circulating heat blanket to maintain body temperature. Vitals, including mucus membrane color, heart rate, respiratory rate, anal temperature, and ambulation, were monitored every 15 minutes through induction and maintenance of anesthesia until the rabbit was fully recovered and alert.

AMD and Glaucoma Model Creation

After baseline imaging, AMD and glaucoma were induced in New Zealand white rabbits through a photocoagulation laser pulsed at 50 ms with a 300 μm diameter that can be used to create localized lesions to the retinal pigment epithelium (RPE) to represent cell atrophy causing vision loss similar to AMD. In the glaucoma model, 4 mg of triescence steroid (40 mg/ml) was injected intravitreally into the vitreous to increase the IOP through a steroid response mechanism.

OCT and PAM

Baseline imaging was conducted and then repeated longitudinally for 30 days following model creation. Anesthetized rabbits were positioned so that the imaging system could observe the area of interest. OCT images were obtained at an acquisition rate of 36 kHz with a lateral resolution of 3.8 μm , axial resolution of 4 μm , and a depth of 1.9 mm using the Ganymede-II-HR OCT system (Thorlabs, Newton, NJ)¹¹. To obtain PAM images, a custom-built ultrasonic transducer was placed on the conjunctiva of the eye. Saline was administered to decrease corneal dehydration and to allow ultrasound signal coupling. PAM images were acquired at 578 nm with 80 nJ, half of the ANSI safety limit of 160 nJ

at 578–650 nm using an OPO nanosecond pulsed laser light (3–5 ns) with a pulse repetition rate of 1 kHz pumped by diode solid-state laser (NT-242; Ekspla, Vilnius, Lithuania). PAM images had a lateral resolution of 4.1 μm and an axial resolution of 37 μm ¹².

Fundus, FA, and ICGA

Baseline imaging was conducted and then repeated longitudinally following model creation. Fundus photography was conducted with the Topcon 50EX imaging system. About 0.2 ml of 10% fluorescein sodium was injected intravenously in the marginal ear vein for FA. Images were taken immediately following the injection. Saline was topically administered to decrease corneal dehydration. For ICGA, 100 μl of ICG contrast (25 mg/3 ml) was delivered intravenously in the marginal ear vein immediately prior to imaging.

Image Analysis

All images were analyzed with Image J and then compiled into a three-dimensional model using Amira software.

Results

Figure 1D depicts the retinal veins through fundus photography. The optic nerve can be visualized on the left side of the image. The fundus image provides insight into the morphology of the retinal vein, running from the bottom left to the top right of the image; however, we are unable to analyze the choroidal vessels. The subsequent FA and ICGA images are better able to visualize the blood flow in the choroid, as seen in the dense region of smaller vessels running perpendicularly to the large retinal vein. In Figure 1B, FA demonstrates the retinal veins, along with the surrounding choroidal vessels. Similar to FA, ICG was also used as an injected contrast agent to visualize the retinal and choroidal vessels on a 2D plane in Figure 1C.

Figures 1E and 1F present a 2D cross section of the retina using OCT. Similar to fundus photography, the OCT images successfully visualize the retinal layers but are limited in their view of the choroidal vessels. The structural layers of the retina, including the RPE, choroid, and sclera, are clearly visualized. At 2.6, 3.1, and 3.4 mm on the x -axis of image x , the retinal veins depicted in Figures 1A–D are visible. Figure 1A shows the x, z plane of these

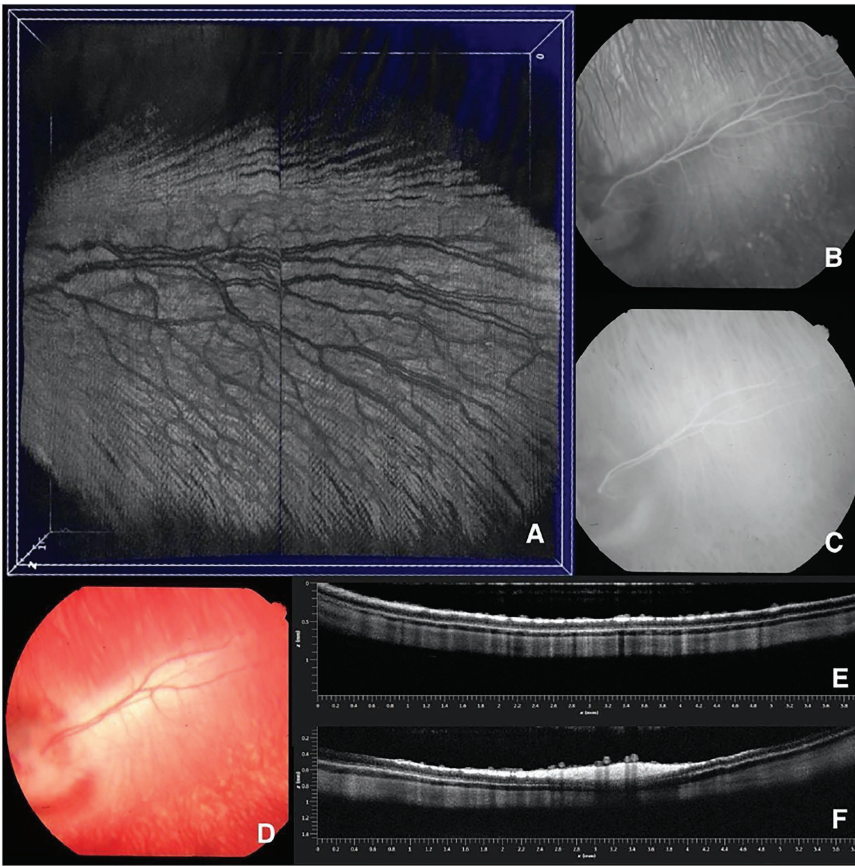


Figure 1: Retinal Imaging of Rabbit: (A) 3D OCT, (B) FA, (C) ICGA, (D) Fundus photography, (E, F) OCT

two images compiled into a 3D OCT scan. The scan spatially visualizes the retinal veins with respect to the choroidal veins.

Discussion

As mentioned in the introduction, each individual modality has its own limitations. Alone, fundus photography is restrained by a lack of image depth and inadequate visualization of the choroidal vessels. When fundus is paired with FA, we can better detect retinal blood flow. Figure 1B shows increased detail in the retinal vein compared to only fundus in Figure 1D. Similarly, when pairing fundus with ICGA, we now observe choroidal blood flow. The brighter-colored area behind the retinal vein in Figure 1C indicates healthy choroidal vessels. All of these modalities lack visualization of retinal layers, so OCT was needed to

observe in vivo morphology. The digital combination of the images from each modality forms the 3D digital construction of the retinal vessel and choroidal vessels seen in Figure 1A. The combination of these imaging systems offsets their individual limitations to form a comprehensive image that no individual system can currently capture.

Longitudinal imaging with this multimodal system can be conducted to monitor for retinal disorders, such as AMD and glaucoma. The disruption of blood flow from retinal and choroidal vein occlusions (RVO and CVO) can lead to the creation of new blood vessels (neovascularization) or vessel leakage. Both neovascularization and leakage are indicators of retinal disorder. For example, an increase in neovascularization of the choroid can often indicate progression of AMD. Early disease diagnosis allows preventative treatment before the onset of symptoms, including irreversible vision loss.

Conclusion

The combination of OCT, fundus photography, FA, and ICGA in the reported images effectively provides a comprehensive image of the retinal model. This multimodal technique offsets the limitations of individual modalities and combines their strengths in an efficient system. The increased detail of these overlaid images could assist clinicians in early retinal disease detection, prior to symptom onset, quickly and noninvasively. In addition, a verified disease model would allow the future exploration of novel treatments, such as regenerative therapies.

Funding Information

This work was supported by the Undergraduate Research Opportunity Program (UROP) and was funded by grants from the National Eye Institute (YMP:1K08EY027458, 1R01EY033000, 1R41EY031219), Fight for Sight—International Retinal Research Foundation (YMP: FFSGIA16002), Alcon Research Institute Young Investigator Grant (YMP), unrestricted departmental support from Research to Prevent Blindness, generous support of from Helmut F. Stern Career Development Professorship in Ophthalmology and Visual Sciences (YMP), and the University of Michigan Department of Ophthalmology and Visual Sciences. This research utilized the Core Center for Vision Research funded by the National Eye Institute (P30 EY007003). We thank Drs. Yuqing Chen and Dongshan Yang and the University of Michigan CAMTraST for their generous donation of rabbits.

References

1. Brown, A., Nguyen, V. P., Wang, X. & Paulus, Y. M. (2022). Multimodal tracking of subretinal ARPE-19 cells labeled with indocyanine green contrast in rabbits for potential AMD treatment. *Investigative Ophthalmology & Visual Science*, 63(7), 4424–F0103.
2. Boyd, K. (2022, July 25). *Glaucoma eye drops*. American Academy of Ophthalmology. Retrieved February 14, 2023, from <https://www.aao.org/eye-health/diseases/glaucoma-eyedrop-medicine>
3. Centers for Disease Control and Prevention. (2020, November 24). Don't let glaucoma steal your sight! Centers for Disease Control and Prevention. Retrieved February 14, 2023, from <https://www.cdc.gov/visionhealth/resources/features/glaucoma-awareness.html>
4. Conlon, R., Saheb, H., & Ahmed, I. I. K. (2017). Glaucoma treatment trends: A review. *Canadian Journal of Ophthalmology*, 52(1), 114–124. <https://doi.org/10.1016/j.jcjo.2016.07.013>
5. Glaucoma surgery: Types, costs & success rates. NVISION Eye Centers. (2022, November 23). Retrieved February 14, 2023, from <https://www.nvisioncenters.com/glaucoma/surgery-and-costs/>
6. Ishikawa, M., Yoshitomi, T., Zorumski, C. F., & Izumi, Y. (2015). Experimentally induced mammalian models of glaucoma. *BioMed Research International*, 1–11. <https://doi.org/10.1155/2015/281214>
7. Venkataraman, K., & Herron, T. (2003). Annual direct cost of illness of age-related macular degeneration in the US: Early estimates of societal burden. *Investigative Ophthalmology & Visual Science*, 44(13), 3089.
8. Liu, X., Liu, T., Wen, R., Li, Y., Puliafito, C.A., Zhang, H.F., & Jiao S. (2015). Optical coherence photoacoustic microscopy for in vivo multimodal retinal imaging. *Optics Letters*, 40 doi: 10.1364/OL.40.001370.
9. Li, Y., Zhang, W., Nguyen, V. P., Khan, N. W., Xia, X., Wang, X., & Paulus, Y. M. (2021). Retinal safety evaluation of photoacoustic microscopy. *Experimental Eye Research*, 202, 108368. doi: 10.1016/j.exer.2020.108368. PMID: 33242491
10. Nguyen, V. P., Li, Y., Henry, J., Qian, T., Zhang, W., Wang, X., & Paulus, Y. M. (2021, August 12). In vivo subretinal ARPE-19 cell tracking using indocyanine green contrast-enhanced multimodality photoacoustic microscopy, optical coherence tomography, and fluorescence imaging for regenerative medicine. *Translational Vision Science & Technology*, 10(10): 10. doi: 10.1167/tvst.10.10.10.
11. Nguyen, V. P., Li, Y., Henry, J., Zhang, W., Wang, X., & Paulus, Y. M. (2020, September 5). High resolution multimodal photoacoustic microscopy and optical coherence tomography visualization of choroidal vascular occlusion. *International Journal of Molecular Sciences*, 21(18):6508. doi: 10.3390/ijms21186508.
12. Nguyen, V. P., Zhu, T., Henry, J., Zhang, W., Wang, X., & Paulus, Y. M. (2022). Multimodal in vivo Imaging of Retinal and Choroidal Vascular Occlusion. *Photonics*, 9(3), 201. <https://doi.org/10.3390/photonics9030201>
13. Ophthalmic Photography. Department of Ophthalmology. (n.d.). Retrieved February 14, 2023, from <https://ophthalmology.med.ubc.ca/patient-care/ophthalmic-photography/>
14. Peiffer, R. L., Pohm-Thorsen, L., & Corcoran, K. (1994). Models in ophthalmology and Vision Research. *The Biology of the Laboratory Rabbit*, 409–433. <https://doi.org/10.1016/b978-0-12-469235-0.50025-7>

15. Rein, D. B., Wittenborn, J. S., Burke-Conte, Z., et al. (2022). Prevalence of age-related macular degeneration in the US in 2019. *JAMA Ophthalmol*, 140(12):1202–1208. doi:10.1001/jamaophthalmol.2022.4401
16. Rein, D. B., Wittenborn, J. S., Zhang, X., et al. (2009). Forecasting age-related macular degeneration through the year 2050: The potential impact of new treatments. *Arch Ophthalmol*, 127(4):533–540. doi:10.1001/archophthalmol.2009.58
17. Rosin, P. L., Marshall, D., Morgan, J. E. (2002). Multimodal retinal imaging: New strategies for the detection of glaucoma. *International Conference on Image Processing*, 3 doi: 10.1109/ICIP.2002.1038923. III-III
18. Schmitt, J. M. (1999). Optical coherence tomography (OCT): A review. *IEEE J. Sel. Top. Quantum Electron*, 5:1205–1215. doi: 10.1109/2944.796348.
19. SD, R. N. R. V. Cost analysis of glaucoma medications. *American Journal of Ophthalmology*. Retrieved February 14, 2023, from <https://pubmed.ncbi.nlm.nih.gov/18154755/>
20. Slakter, J. S., Yannuzzi, L. A., Guyer, D. R., Sorenson, J. A., & Orlock, D. A. (1995). Indocyanine-green angiography. *Current Opinion in Ophthalmology*, 6:25–32.
21. Sramek, C., Paulus, Y. M., Nomoto, H., Huie, P., & Palanker, D. (2009). Computational model of retinal photocoagulation and rupture. *Ophthalmic Technologies XIX*. <https://doi.org/10.1117/12.808556>
22. Wang, Z., Feng, C., Yang, R., Liu, T., Chen, Y., Chen, A., Yan, B., Yuan, Y., & Zhang, J. (2021). Large-area photoreceptor degeneration model in rabbits by photocoagulation and oxidative stress in the retina. *Frontiers in Neuroscience*, 15. <https://doi.org/10.3389/fnins.2021.617175>
23. Zhang, W., Li, Y., Nguyen, V. P., Huang, Z., Liu, Z., Wang, X., & Paulus, Y. M. (2018). High-resolution, in vivo multimodal photoacoustic microscopy, optical coherence tomography, and fluorescence microscopy imaging of rabbit retinal neovascularization. *Light: Science & Applications*, 7:103. doi: 10.1038/s41377-018-0093-y.
24. Zhang, W., Li, Y., Yu, Y., Derouin, K., Qin, Y., Nguyen, V. P., Xia, X., Wang, X., & Paulus, Y. M. (2020, June 6). Simultaneous photoacoustic microscopy, spectral-domain optical coherence tomography, and fluorescein microscopy multi-modality retinal imaging. *Photoacoustics* 20: 100194. <https://doi.org/10.1016/j.pacs.2020.100194>